Direct Measurement of Reconnection Outflow Profile by Glass-Tube-Pair Type Doppler Probes in Tokamak Merging Experiments

Ryo SOMEYA*, Luo JIAXIAO, Yunhan CAI, Tara AHMADI, Hiroshi TANABE, Yasushi ONO

Graduate School of Frontier Sciences, The University of Tokyo, Tokyo 113-0032, Japan

(Received 21 April 2025 / Accepted 20 June 2025)

The reconnection outflow velocity under high guide field was directly measured using the 1D array of ion Doppler probes and was compared with the $E \times B$, gradient B, and curvature drift velocity calculated from 2D profile measurements of electric and magnetic fields for the first time. It was found that the measured ion velocity profile agrees well with the profile of $E \times B$ drift velocity which is much larger than the other drift velocities. The poloidal flux-line velocity is almost equal to the $E \times B$ drift and ion flow velocities, probably because magnetic flux is almost frozen into ions due to its large Lundquist number of 10^2.

Keywords: merging tokamaks, magnetic reconnection, ion outflow, Doppler spectroscopy, ion drift velocity

DOI: 10.1585/pfr.20.1402041

1. Introduction

Magnetic reconnection is attractive as ion heating method in fusion plasmas. University of Tokyo and Tokamak Energy Inc. have been using merging spherical tokamak plasmas for startup and heating for future fusion plasma ignition [1–3]. In general, magnetic reconnection effectively converts reconnecting magnetic energy into the particle energy and are observed also in solar flares, magnetopause and sawtooth crashes in tokamaks [4–6]. Since most of the released magnetic energy are transferred to ion energy [7], ion acceleration mechanisms are crucial for understanding the physics of reconnection. According to recent studies, ions are heated mainly by fast shock or viscous damping of the reconnection outflow in the downstream areas, while electrons are heated inside the current sheet mainly by the Ohmic heating [8]. The ion heating energy is proportional to B_p^2 and ion outflow speed is about 70% of poloidal Alfvén speed [8, 9]. The ion outflow should be ion drift motion, because ions are fully magnetized in merging tokamaks whose toroidal magnetic field about 10 times larger than the reconnecting magnetic field. Then an important question arise as to which drift velocity causes the reconnection outflow. Direct acceleration of ions by reconnection electric field around X-point also exists and substantial toroidal ion flow had been observed [10], but the significant ion heating of 50–70 eV is observed mainly in the downstream region, and since this structure is consistent with the ion outflow structure [8], the outflow is considered as the primary cause for the ion heating. For ion velocity measurements, ion Doppler spectroscopy is one of the most reliable methods in both laboratory experiments and space observations [11, 12]. Since the measured line spectral emission from bulk plasma is integrated along the viewing line, direct Doppler probe measurement [13] or Doppler tomographic reconstruction [14] is required for spatial profile measurements. The Doppler probe can directly measure local ion flow [13], but the large probe size causes large plasma perturbation. The reconstruction methods can measure ion temperature profile successfully [14], but it is still difficult to reconstruct local ion flow. It is because the vector tomography, which has been established in theory and numerical simulations [15], requires high spatial resolution spectroscopy from multiple directions. However, the current resolution of spectroscopy is not sufficient to detect the line-averaged Doppler shift, which is too small to reconstruct outflow profile in experiments. Using a glass-tube-pair type Doppler probes, we realized a direct 1D/two-component measurement of ion flow profile with low plasma perturbation, and it revealed that ion outflow of two merging spherical tokamak plasmas is about 70% of poloidal Alfvén speed in agreement with recent reconnection experiments and theory [9, 16].

To clarify the mechanisms of the ion outflow formation in merging tokamaks reconnection, we focused on ion drift motion under high toroidal magnetic field—about 10 times larger than the reconnection magnetic field. The ion mean velocity $\boldsymbol{v}_i$ is expected to be equal to ion drift velocity $\boldsymbol{v}_{i,drift}$ described as follows:

$$\boldsymbol{v}_i \simeq \boldsymbol{v}_{i,drift} = \boldsymbol{F} \times \frac{\boldsymbol{B}}{q_i B^2}, \tag{1}$$

*Corresponding author's e-mail: rsomeya@ts.t.u-tokyo.ac.jp

where $\boldsymbol{F}$, $\boldsymbol{B}$ and q_i are drift force, magnetic field, and charge of ion, respectively [17]. The drift force $\boldsymbol{F}$ is mainly expressed as

$$\boldsymbol{F} = q_i\boldsymbol{E} + \left(-\frac{m_i v_{i,L}^2}{2B}\nabla\boldsymbol{B}\right) + \frac{m_i v_{i,gc}^2}{R_c}\boldsymbol{n}_{R_c}, \tag{2}$$

where $\boldsymbol{E}$, m_i, $v_{i,L}$, $v_{i,gc}$, R_c and $\boldsymbol{n}_{R_c}$ are electric field, ion mass, ion Larmor orbit velocity, ion guiding center velocity, curvature radius of magnetic field lines and unit vector of R_c respectively [17]. The first term is electrostatic force, the second term is magnetic gradient force, and the third term is magnetic centrifugal force. Therefore, using measurements of ion mean velocity, electric field and magnetic field measurement, ion outflow profile can be compared with ion drift velocity profile. In this article, we used three types of probe measurements which can measure 1D profile of ion velocity $v_{i,r}$ and $v_{i,z}$, and 2D profile of electric and magnetic field and compared the ion outflow profile with ion drift velocity profile to study the mechanisms for ion outflow formation in two merging tokamaks reconnection. Particle drifts do not directly mean ion outflow, but our ion velocity measurement measures all of ion velocities using the line-spectrum emission. We estimated all of ion drifts velocities and compared the measured ion velocity with them as candidates for the reconnection outflow.

2. Glass-Tube-Pair Type Doppler Probes

Figure 1(a) shows the internal structure of our glass-tube-pair type Doppler probes which we have developed [9, 16]. Just a pair of straight glass tubes with an outer diameter of 10 mm are inserted into two merging plasmas for ion outflow profile measurement of the rectangular area between the two parallel tubes. By scanning the probes in the r direction, the interval between measurement points can be shortened. Each measurement volume (32 mm × 25 mm × 10 mm) is surrounded by 4 first surface mirrors (3 mm × 3 mm × 1 mm) and 4 optical fibers with a clad diameter of 500 μm, which are installed with mirror holders made by stereolithography (SLA) 3D printer. Numerical aperture of the optical system is measured as 0.10 in preliminary experiments with a light source in front of the probe. This means that the structure in the opposing glass tube can completely block the emission from the ions behind the opposing tube. Our probes measure line spectra emitted from ions along a pair of viewing lines: 1-A & 1-B and the other two viewing lines which are inclined to 1-A by the angle of 30° (1-C) or 150° (1-D). For 1D profile measurement, 7 sets of mirrors and optical fibers are aligned in the two parallel glass tubes. All 4 × 7 optical fibers are led in a row to a Czerny-Turner spectrometer and finally to an Intensified Charge Coupled Devices (ICCD) camera for Doppler spectra measurements with an exposure time of 4 μs [11]. Using Doppler shift measurements from bi-directional viewing lines 1-A & 1-B, we can significantly decrease the calibration error of the Doppler shifts [9, 16]. From Doppler shifts in viewing lines 1-C & 1-D, $\Delta\lambda_C$ and

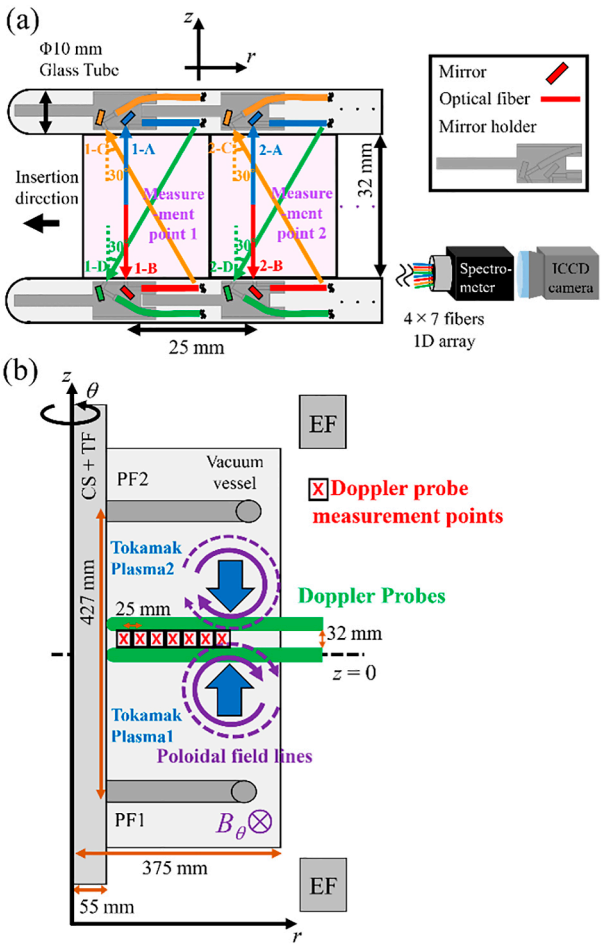

Fig. 1. (a) Schematic view of ion flow profile measurement system composed of glass-tube-pair type Doppler probes and the optical system [16], (b) schematic view of magnetic field lines of two merging tokamak plasmas and Doppler probes in TS-6 [18].

$\Delta\lambda_D$, viewing direction (orange and green arrows) components of ion mean velocity $v_{i,C}$ and $v_{i,D}$ are calculated as follows:

$$v_{i,C} = -\frac{\Delta\lambda_C}{\lambda_0}c,\ v_{i,D} = -\frac{\Delta\lambda_D}{\lambda_0}c, \tag{3}$$

where c, and λ_0 are light speed and spectral line wavelength, respectively. By use of two velocity components in two different directions, ion mean velocity vectors in r-z plane $v_{i,r}$ and $v_{i,z}$ can be calculated for each measurement volume as follows:

$$\begin{pmatrix} v_{i,C} \\ v_{i,D} \end{pmatrix} = \begin{pmatrix} \cos 30^\circ & -\sin 30^\circ \\ -\cos 30^\circ & -\sin 30^\circ \end{pmatrix} \begin{pmatrix} v_{i,z} \\ v_{i,r} \end{pmatrix}, \tag{4}$$

$$\therefore \begin{cases} v_{i,z} = \dfrac{1}{2\cos 30^\circ}(v_{i,C} - v_{i,D}) \\ v_{i,r} = -\dfrac{1}{2\sin 30^\circ}(v_{i,C} + v_{i,D}) \end{cases}. \tag{5}$$

The Doppler probes system was installed in the TS-6 device [18], whose cylindrical vacuum vessel with a diameter of 0.75 m and axial length of 1.44 m, has two internal Poloidal Field (PF) coils at z = ± 0.2135 m. Two tokamak

plasmas are produced by induction of those PF coils. When the coil currents reverse, the two tokamaks are fully pinched off from them and move toward the mid-plane to merge together. Figure 1(b) shows the experimental setups of the probes in a TS-6 device. Two glass tubes were inserted into the vacuum vessel radially at z = 0 and 0.042 m to measure the radial profile (r = 0.1, 0.125, 0.15, 0.175, 0.2, 0.225, and 0.25 m) of ion velocity at z = 0.021 m.

3. 2D Electric and Magnetic Fields Measurements by Probes

For 2D profile of magnetic field measurement, we used printed-circuit board (PCB) coil probe array [19]. Each coil printed on a circuit board had a cross-sectional area of 3 mm × 5 mm and 19 turns. Each probe array composed of ten printed coils was installed in a straight glass tube with outer diameter of 5 mm. They were located at 0.03 m intervals from r = 0.06 to 0.33 m. Those probe arrays were inserted into the r-z planes different from Doppler probes and their positions were at z = ± 0.01, ± 0.03, ± 0.085, ± 0.128 and ± 0.17 m respectively. Time evolutions of dB_z/dt signals measured by those probe arrays were led to integral amplifier circuits and were transformed into time evolution of B_z at the coil positions. With these data and the cylindrical symmetry assumption, 2D profile of magnetic field B_r and poloidal flux Ψ can be calculated as follows:

$$\Psi = \int 2\pi r B_z dr, \tag{6}$$

$$B_r = -\frac{1}{2\pi r}\frac{\partial \Psi}{\partial z}. \tag{7}$$

As the CS + TF coils provide a good conductor surface, Ψ on r = 0.055 m can be assumed to be zero. Also, toroidal current density j_θ and toroidal electric field E_θ were calculated using the following Ampere's law and Faraday's law respectively:

$$j_\theta(R,z) = \frac{1}{\mu_0}\left[\frac{\partial B_r}{\partial z} - \frac{\partial B_z}{\partial r}\right]_{r=R}, \tag{8}$$

$$E_\theta(R,z) = -\frac{1}{2\pi R}\frac{\partial \Psi}{\partial t}\bigg|_{r=R}. \tag{9}$$

Our pick-up coil measurement indicates that the toroidal field produced by the plasma is less than 3% of that produced by the external Toroidal Field (TF) coil during merging tokamaks. Therefore, the toroidal field in merging experiments B_θ was almost equal to vacuum field as follows:

$$B_\theta(R,z) \simeq \frac{\mu_0 I_{TF}}{2\pi R}, \tag{10}$$

where I_{TF} is TF coil current. Figure 2(a) shows time evolution of 2D profile of toroidal current density (colormap) and poloidal magnetic flux (lines) in Argon tokamak merging experiments with electron density of 2 ~ 5 × 10^{19} m^{-3} measured by

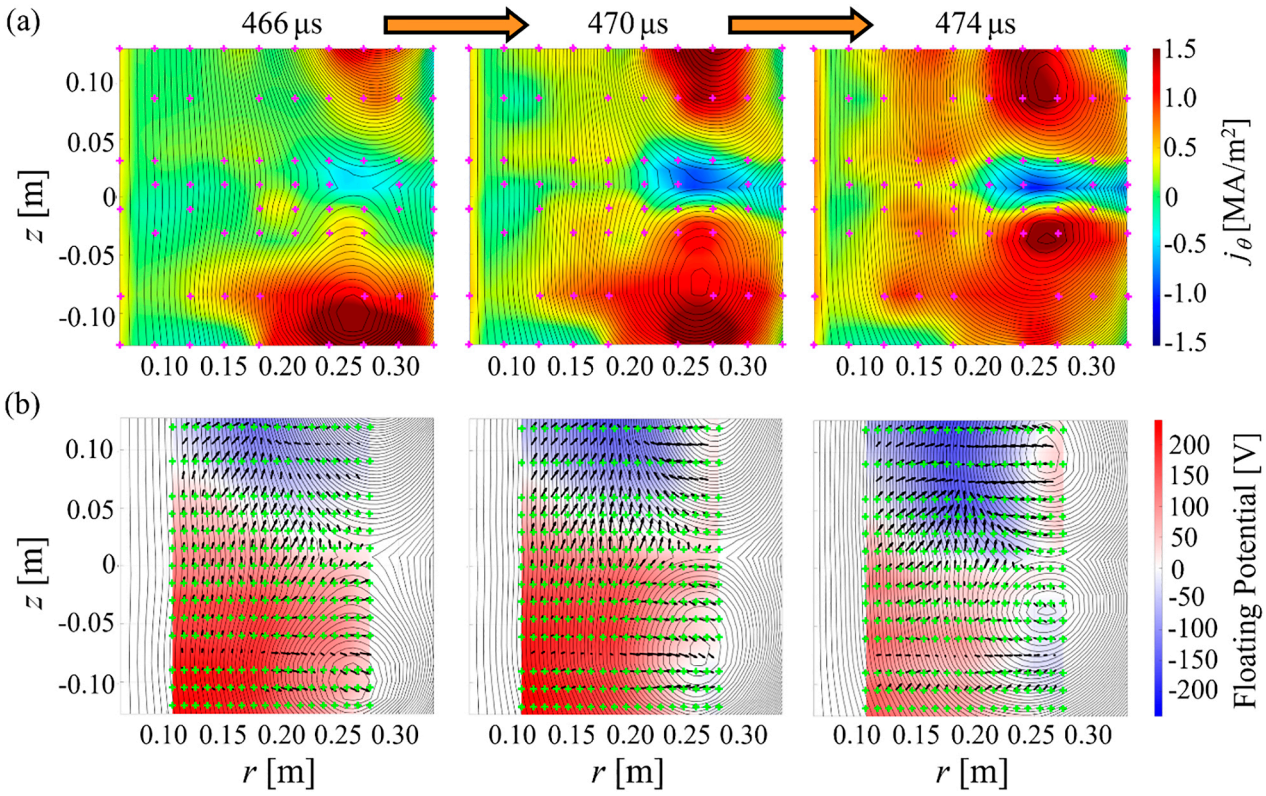

Fig. 2. (a) 2D profiles of toroidal current density (color) and poloidal magnetic flux (lines) with measurement points of PCB magnetic probes (magenta crosses), (b) 2D profiles of floating potential (color), poloidal electrostatic field (black arrows), and poloidal flux (lines) with measurement points of electrostatic potential probe (green crosses).

the triple probe [20]. TF coil current, maximum PF coil current and gas fill pressure were set to 2.1×10^2 kA × Turn, 1.1×10^2 kA × Turn, 1.1 mTorr respectively and upstream reconnecting field was about 30 mT. We did not use Center Solenoid (CS) coil current drive in this experiment. The magenta crosses indicate measurement points of PCB magnetic probes. The outflow region where ion outflows are generated is distributed around the X-point with a width larger than the current sheet width in the z direction [21]. To generate the outflow region in the measurement volume of Doppler probes around z = 0.021 m, discharge times of PF1 and PF2 coils were set to 400 and 405 μs, respectively and the center of the outflow region was successfully moved to z = 0.015 m while confirming that the merging surface was not tilted. As shown in Fig. 2(a), the reversed PF coil current push two tokamak plasmas together in the vertical direction, forming current sheet on the midplane.

For 2D profile of electric field measurement, we used 1D array of electrostatic probes in the z direction [22, 23]. There are 21 probes covered by insulation tubes at intervals of 0.015 m from z = −0.15 to 0.15 m and can measure the axial (z) profile of floating potential in single shot using the following formula:

$$\phi_f = \phi_{plasma} - \frac{kT_e}{e}\ln\sqrt{\frac{m_i}{4\pi m_e}}, \tag{11}$$

where ϕ_f, ϕ_{plasma}, T_e and m_e are floating potential, plasma potential, electron temperature and electron mass, respectively [22]. Using radial scan of the probe array from r = 0.105 to 0.285 m, we measured 2D profile of floating potential. Since Thomson scattering system has observed electron temperature gradient only in the vicinity of the X-point [24], poloidal electrostatic field $\boldsymbol{E}_p$ approximates as follows:

$$\boldsymbol{E_p} = -\nabla\phi_{plasma} \simeq -\nabla\phi_f\,. \tag{12}$$

The inductive poloidal electric field measured by pick-up coil is negligibly small in comparison with the poloidal electrostatic field. Figure 2(b) shows time evolution of 2D profile of floating potential (colormap), poloidal electrostatic field (black arrows), poloidal magnetic field lines (contour plot) and measurement points of electrostatic potential probe (green crosses) in the same experiments as Fig. 2(a). It is observed that quadrupole electrostatic potential is formed as the two tokamaks merge. This result is consistent with the results of previous studies [22, 25–27].

In addition to the measured electromagnetic field results presented above, ion Larmor orbit velocity $v_{i,L}$ and ion guiding center velocity $v_{i,gc}$ were required for the calculation of drift forces. Since typical toroidal magnetic field strength is about 0.2 T, singly charged Argon ions with temperature of 10 eV have about 1 cm Larmor radius, which is small enough to use guiding center assumption. The ion thermal velocity was obtained from ion temperature of 10 eV, which is a typical value estimated from the Doppler tomography system [18] measurement results under similar condition. Theoretically, the guiding center velocity should be calculated from the electric field parallel to the total magnetic field, but under conditions where the toroidal field is sufficiently large compared to the poloidal field, the guiding center velocity can be approximated as almost parallel to toroidal direction and accelerated by a toroidal electric field. From the above discussion, the toroidal component of guiding center velocity $v_{i,gc,\theta}$ was approximated as follows:

$$v_{i,gc,\theta} \simeq \frac{1}{m_i}\int q_i E_\theta dt\,. \tag{13}$$

The integration time starts at 460 μs, when toroidal electrostatic field appears and ends at 470 μs. Since the ion-electron collision frequency in our case is about 10^4 Hz, ion-electron collision term can be negligible during toroidal acceleration by reconnection electric field. Also, since the guiding center velocity is parallel to the magnetic field, the total guiding center velocity was calculated as follows:

$$v_{i,gc} = v_{i,gc,\theta} \times \frac{B}{B_\theta}\,. \tag{14}$$

4. Comparison of Ion Velocity and Ion Drift Velocity during Merging Tokamaks Reconnection

Using measured 2D profile of electromagnetic field and these assumptions above, we obtained poloidal component of drift force profile in the downstream region as shown in Fig. 3(a) (470 μs). Focusing on the slope of the arrow in Fig. 3(b), the r component of electrostatic force in the upstream region, is about three times larger than the z component, while the z component in the downstream is about ten times larger than the r component, which is related with the characteristics of quadrupole electrostatic potential. As shown in Figs. 3(c) and (d), the magnetic gradient and the magnetic centrifugal force is almost parallel to r direction and the r component of magnetic gradient force is determined mostly by the gradient of toroidal magnetic field, which increases inversely with r. On the other hand, the r component of the magnetic curvature force is zonally highly distributed between r = 0.14 and 0.18 m, presumably due to the high curvature of toroidal magnetic field and the high guide center velocity here. Also, there are larger z components in the upstream region, where the z directional gradient and curvature of the reconnection magnetic field are larger than in the downstream region. Comparing absolute values of the three forces, electrostatic forces are about two orders of magnitude larger than the other two forces. Therefore, the $E \times B$ drift is the dominant ion drift velocity in this high guide field reconnection of two merging tokamak plasmas.

Figure 4 shows radial profile of ion velocity measured by the Doppler probe array and ion drift velocity calculated from the drift forces at z = 0.021 m and 470 μs. The interval between measurement points of ion flow was shortened by scanning the Doppler probe in the r direction under identical conditions. No adrupt change in z component of ion mean velocity were observed around r = 0.20 m, where r component

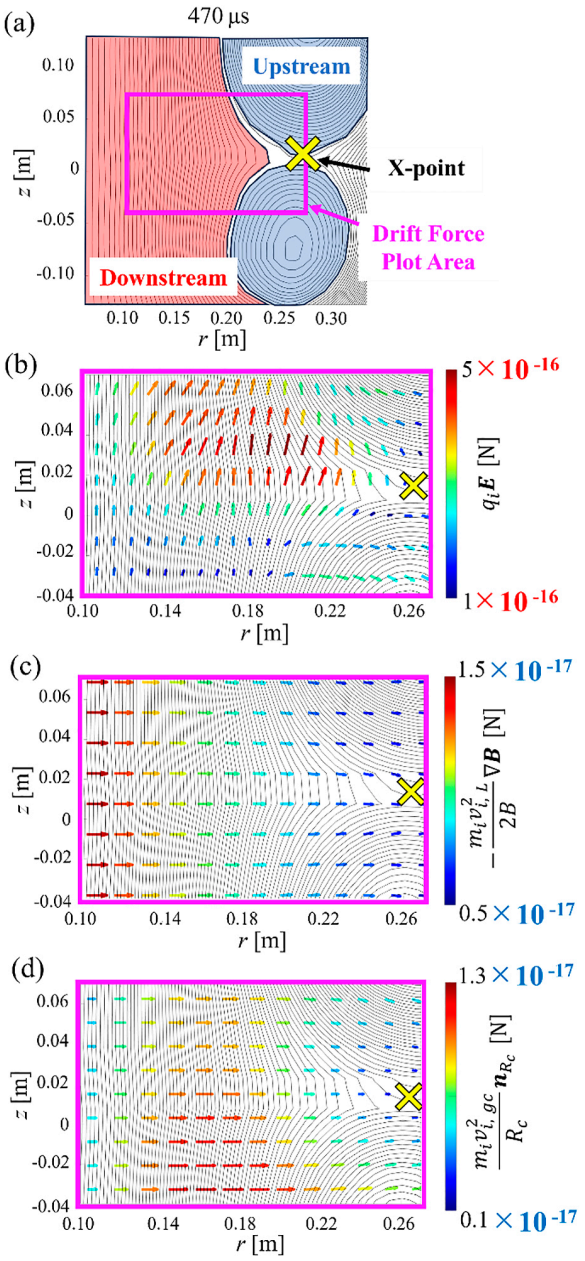

Fig. 3. (a) Global poloidal flux contour of two merging tokamak plasmas on *r*-*z* plane at 470 μs, 2D profiles of (b) electrostatic forces, (c) magnetic gradient forces, and (d) magnetic centrifugal forces at 470 μs.

of the velocity decreased rapidly, and was considered to be fast-shock. In addition to confirming that the main component of ion drift is $E \times B$ drift, the profile of $E \times B$ drift is in good agreement with the profile of ion flow. The poloidal flux-line velocity v_Ψ profiles, shown in the green curve, were estimated from the time variation of the position of poloidal flux Ψ contours in the downstream area based on zero resistivity assumption. The specific calculation method of v_Ψ is as follows. The time variation of the radial profile of poloidal flux $\Psi(r,t)$ on z = 0.021 m is known. To calculate the velocity at $(r, t) = (r_0, t_0)$, r_1 and r_2 satisfying $\Psi(r_0,t_0) = \Psi(r_1,t_0-\Delta t) = \Psi(r_2,t_0+\Delta t)$ are identified, where Δt is the time resolution of magnetic field measurement of 1 μs. Then

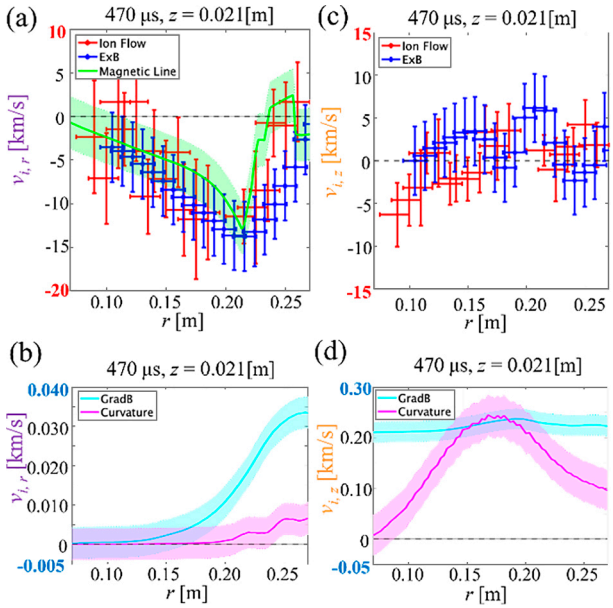

Fig. 4. (a) and (b) Radial profiles of radial ion flow, $E \times B$ drift, gradient B drift, curvature drift velocities and Ψ contour velocity at z = 0.021 m and 470 μs, (c) and (d) radial profile of axial ion flow, $E \times B$ drift, gradient B drift and curvature drift velocities at z = 0.021 m and 470 μs.

v_Ψ can be calculated as follows:

$$v_\Psi(r_0,t_0) = \frac{r_2 - r_1}{2\Delta t}. \tag{15}$$

This profile also agrees well with the $E \times B$ drift and ion flow profiles, because magnetic flux lines are almost frozen into ions. Lundquist number S is the ratio of magnetic diffusion time to the Alfvén time and defined as follows:

$$S = \frac{\mu_0 v_A L}{\eta}, \tag{16}$$

where v_A, L and η are Alfvén speed, typical scale length and magnetic diffusivity [17]. In our experiments, with large Lundquist number of 10^2, the effect of magnetic diffusion is so small that magnetic flux lines are almost frozen into ions. The magnetic dissipation time calculated from maximum psi damping ratio, is about 3 × 10 μs, which is much longer than flux transfer time scale. On z = 0.021 m, normalised density gradient $\nabla n/n$ can be estimated to be less than 1/0.1 m^{-1} in the r direction, and the ion diamagnetic drift velocity is estimated to be less than 0.3 km/s in the z direction. This value is comparable to the gradient B and curvature drift, but is much smaller than the measured $E \times B$ drift. The diamagnetic drift does not affect the conclusion that the ion flow is caused by the $E \times B$ drift. When the convective derivative of the drift velocity is sufficiently large, ion polarization drift should be taken into account. However, the ion polarization drift velocity is calculated to be as negligibly small as 3 × 10^{-3} km/s in the downstream region at 470 μs.

5. Conclusion

In summary, we have studied the mechanisms for ion outflow formation during magnetic reconnection of two merging tokamaks with $B_\theta/B_p \sim 10$ by comparing ion outflow velocity profile with ion drift velocity profiles under fully magnetized condition. We measured the reconnection outflow characteristics using three direct measurements by the 1D array of ion Doppler probes, the 2D array of PCB magnetic probes and the 1D array of electrostatic probes. Using 1D profile of ion flow and 2D profiles of electric and magnetic field, we compared the measured ion outflow profile with the ion drift velocity profiles in downstream region for the first time. We calculated the drift forces in downstream region and found that $E \times B$ drift is the dominant ion drift velocity in this high guide field reconnection of two merging tokamak plasmas. Furthermore, we compared ion flow profile with ion drift velocity profile and discovered that the measured ion velocity profile agrees well with the profiles of $E \times B$ drift velocity. The poloidal flux-line velocity estimated from the time variation of the position of poloidal flux contours, also agrees well with the $E \times B$ drift and ion flow profiles, probably because magnetic flux is almost frozen into ions due to large Lundquist number of 10^2.

Acknowledgements

This works was supported by Grant-in-Aid for Scientific Research 22J20382, 22KJ1009, 15H05750, 15K14279, 17H04863 and 18K18747.

[1] M. Yamada *et al.*, Rev. Mod. Phys. **82**, 603 (2010).
[2] M.P. Gryaznevich and A. Sykes, Nucl. Fusion **57**, 072003 (2017).
[3] Y. Ono *et al.*, Phys. Plasmas **22**, 055708 (2015).
[4] K. Shibata, Astrophys. Space Sci. **264**, 129 (1998).
[5] H.U. Frey *et al.*, Nature **426**, 533 (2003).
[6] M. Yamada *et al.*, Phys. Plasmas **1**, 3269 (1994).
[7] M. Yamada *et al.*, Nat. Commun. **5**, 4774 (2014).
[8] Y. Ono *et al.*, Phys. Rev. Lett. **107**, 185001 (2011).
[9] R. Someya *et al.*, Plasma Fusion Res. **16**, 1202078 (2021).
[10] A. Goodman *et al.*, Phys. Plasmas **30**, 112104 (2023).
[11] H. Tanabe *et al.*, Nucl. Fusion **53**, 093027 (2013).
[12] H. Hara *et al.*, Astrophys. J. **741**, 107 (2011).
[13] A. Kuritsyn *et al.*, Rev. Sci. Instrum. **77**, 10F112 (2006).
[14] A.L. Balandin and Y. Ono, Eur. Phys. J. D **17**, 337 (2001).
[15] A.L. Balandin *et al.*, Comput. Math. Appl. **63**, 1433 (2012).
[16] R. Someya *et al.*, Phys. Plasmas **30**, 060701 (2023).
[17] P.M. Bellan, Fundamentals of Plasma Physics (Cambridge University Press, Cambridge, 2008).
[18] H. Tanabe *et al.*, Nucl. Fusion **59**, 086041 (2019).
[19] M. Akimitsu *et al.*, Plasma Fusion Res. **13**, 1202108 (2018).
[20] S.-L. Chen and T. Sekiguchi, J. Appl. Phys. **36**, 2363 (1965).
[21] Y. Ono *et al.*, Plasma Phys. Control. Fusion **54**, 124039 (2012).
[22] K. Yamasaki *et al.*, Phys. Plasmas **22**, 101202 (2015).
[23] H. Tanaka *et al.*, IEEJ Trans. Fundam. Mater. **143**, 63 (2023).
[24] X. Guo *et al.*, Phys. Plasmas **22**, 101201 (2015).
[25] J. Egedal *et al.*, Phys. Plasmas **16**, 050701 (2009).
[26] N. Katz *et al.*, Phys. Rev. Lett. **104**, 255004 (2010).
[27] W. Fox *et al.*, Phys. Rev. Lett. **118**, 125002 (2017).